Journal of Alloys and Compounds 509 (2011) 6433–6439

Contents lists available at ScienceDirect

Journal of Alloys and Compounds

journal homepage: www.elsevier.com/locate/jallcom

# Temperature dependent current–voltage and capacitance–voltage characteristics of chromium Schottky contacts formed by electrodeposition technique on n-type Si

Ö. Demircioglu[a], Ş. Karataş[b,*], N. Yıldırım[c], Ö.F. Bakkaloglu[a], A. Türüt[d]

[a] Department of Engineering Physics, Faculty of Engineering, University of Gaziantep, 27310 Gaziantep, Turkey
[b] Department of Physics, Faculty of Sciences and Arts, University of Kahramanmaraş Sütçü İmam, 46100 Kahramanmaraş, Turkey
[c] Department of Physics, Faculty of Sciences and Arts, Bingöl University, 12100 Bingöl, Turkey
[d] Atatürk University, Faculty of Sciences and Arts, Department of Physics, 25240 Erzurum, Turkey

ARTICLE INFO

*Article history:*
Received 25 June 2010
Received in revised form 11 March 2011
Accepted 15 March 2011
Available online 21 March 2011

*Keywords:*
Schottky barrier inhomoheneities
Si
*I–V–T* and *C–V–T* characteristics

ABSTRACT

The variations in the electrical properties of Cr Schottky contacts formed by electrodeposition technique on n-type Si substrate have been investigated as a function of temperature using current–voltage (*I–V*) and capacitance–voltage (*C–V*) measurements in the temperature range of 80–320 K by steps of 20 K. The basic diode parameters such as ideality factor ($n$) and barrier height ($\Phi_b$) were consequently extracted from the electrical measurements. It has been seen that the ideality factor increased and the barrier height decreased with decreasing temperature, when the *I–V* characteristics were analyzed on the basis of the thermionic emission (TE) theory. The abnormal temperature dependence of the $\Phi_b$ and $n$ and is explained by invoking two sets of Gaussian distribution of barrier heights at 320–200 K, and 180–80 K. The double Gaussian distribution analysis of the temperature-dependent *I–V* characteristics of the Cr/n-type Si Schottky contacts gave the mean barrier heights of 0.910 and 0.693 eV and standard deviations ($\sigma_s$) of 109 mV and 72 mV, respectively. Then, these values of the mean barrier height have been confirmed with the modified $\ln(I_0/T^2) - q^2/2k^2T^2$ versus $1/T$ plot which belongs the two temperature regions.


## 1. Introduction

Si has many industrial uses, and it is the principal component of most semiconductor devices, importantly integrated circuits or microchips. Metal film deposition on Si semiconductor has received much attention for the fabrication of optoelectronics, microwave devices, and integrated circuits used in modern high-sped optical system. Thus, due to the technological importance of metal-semiconductor Schottky contacts, a full understanding of their current–voltage (*I–V*) and capacitance–voltage (*C–V*) characteristics are of great interest [1–9]. Schottky contacts with low barrier height find applications in devices operating at cryogenic temperatures such as infrared detectors, sensors in thermal imaging, microwave diodes, gates of transistors and infrared and nuclear particle detectors [10–14].

The *I–V* characteristics of the metal-semiconductor (MS) contacts usually deviate from the ideal thermionic emission (TE) current model [15]. Therefore, the analysis of the *I–V* characteristics of the Cr/n-type Si Schottky contacts at room temperature only does not give detailed information about their conduction process or the nature of barrier formation at the MS interface [15–18]. Moreover, the temperature dependence of the *I–V* characteristics allows us to understand different aspects of conduction mechanisms across the MS interface and the study of different effects such as barrier inhomogeneities and surface states density on carrier transport at MS Schottky contacts [19–23]. The analysis of the *I–V* characteristics of SBDs based on the TE theory usually reveals an abnormal decrease in the BH $\Phi_b$ and an increase in the ideality factor $n$ with decreasing temperature [1–4,15]. The decrease in the barrier height at low temperatures in fact leads to nonlinearity in the activation energy ($\ln(I_0/T^2)$ versus $1/T$) plot. We can roughly categorize the conduction mechanisms into three types: (1) thermionic emission (TE) over the barrier, (2) field emission (FE) near the Fermi level, and (3) thermionic-field emission (TFE) at energy between TE and FE. While FE is a pure tunneling process, TFE is tunneling of thermally excited carriers which see a thinner barrier than FE. The relative contributions of these components depend on both temperature and doping level.

Many experimental and theoretical studies of the current flow mechanism in Schottky barriers have been reported in the literature [2,6,10–12,23–26]. For example, Hasegawa et al. [27,28] have characterized both experimentally and theoretically electri-

* Corresponding author. Tel.: +90 344 219 1310; fax: +90 344 219 1042.
*E-mail address:* skaratas@ksu.edu.tr (Ş. Karataş).

0925-8388/$ – see front matter © 2011 Elsevier B.V. All rights reserved.
doi:10.1016/j.jallcom.2011.03.082

cal properties of nanometer-sized Schottky contacts which are successfully formed on n-GaAs and n-InP substrates by a combination of an electrochemical process and an electron-beam (EB) lithography. They [27,28] have proved that nanometer-sized Schottky contacts formed by in situ electrochemical process are an efficient approach to Schottky limit for metal/III–V junctions (very large SBH of 0.86 eV) due to reducing Fermi level pinning. In particularly, in the past few decades, some researchers have reported noteworthy works for physical and chemical properties of semiconductors like GaAs, Si, InP, etc. [10–14,27–34]. Güzeldir et al. [13] studied the *I–V* and *C–V* characteristics of this Zn/ZnSe/n-Si/Au–Sb structure in wide temperature range by 20 K steps. Sharma [29] studied forward current–voltage characteristics of the Au/n-Si Schottky barrier diodes in the temperature range of 70–310 K. Nuhoğlu and Gülen [30] determined the current–voltage and capacitance–voltage characteristics of n-Si Schottky barrier diode in the temperature range of 100–800 °C. Tatar et al. [33] were investigated the electrical properties of the Cr/p-Si(1 1 1) and Cr/n-Si(1 0 0) junctions were investigated through *C–V* and *I–V* measurements, performed under dark and light conditions at room temperature. Besides, Zhou et al. [34] studied the electrical characteristics of Schottky rectifiers with a $SiO_2$ field plate on a free standing n-GaN in the temperature range of 298–473 K.

In this study, the *I–V* and *C–V* characteristics of Cr Schottky contacts formed by electrodeposition technique on n-type Si substrate were measured over the temperature range of 80–320 K by steps of 20 K. The reason why metal Cr is used as the Schottky contacts in this study is the work function of Cr which is lower than that of usually used metals such as Ni, Au, Co and Pt, and also it is more interactive than these metals. In addition, since Ni, Au, Co and Pt are high refractory metals, it is not practical to deposit thick layers of Ni, Au, Co or Pt by electron beam evaporation. Furthermore, metal Cr on Si is expected to form a large barrier Schottky contact due to its high work function [24]. Thus, metal Cr can be preferred to other metals (like Ni, Au, Co and Pt) for Schottky contact. The analysis of the forward-bias characteristics of the devices based on the TE mechanism have revealed an abnormal decrease of $\Phi_b$ and increase of $n$ with decreasing temperatures, and these changes become effective especially at low temperatures. The temperature dependent barrier characteristics of the Cr/n-type Si Schottky contacts were interpreted by using a double-Gaussian spatial distribution of BHs. Furthermore, the series resistance effect was observed in the *I–V* characteristics.

## 2. Experimental procedures

The n-type Si wafer used in this study was (1 0 0) oriented and with the free carrier concentration of $1.25 \times 10^{15}$ $cm^{-3}$ from the reverse bias $C^{-2}$–*V* characteristics at room temperature. The wafers were chemically cleaned using the RCA cleaning procedure [i.e., a 10 min boil in $NH_4OH + H_2O_2 + 6H_2O$ followed by a 10 min boil in $HCl + H_2O_2 + 6H_2O$]. The native oxide on the front surface of the substrates was removed in $HF:H_2O$ (1:10) solution and finally the wafer was rinsed in de-ionized water for 30 s. Then, low resistivity ohmic back contact to the n-type Si wafer was made by using Au–Sb alloy, followed by a temperature treatment at 420 °C for 3 min in $N_2$ atmosphere. The electrodeposition of Cr Schottky contacts of the n-Si substrate was carried out in the galvanostatic mode from an electrolyte containing $CrO_3$ (250 g/l) and $H_2SO_4$ (2.5 g/l) at room temperature, and the Schottky contacts were formed on the front face of the n-Si as dots with diameter of about 1 mm (the diode area = $7.85 \times 10^{-3}$ $cm^2$) by the galvanostatic electrodeposition of Cr. An acid resistant adhesive tape was used to mask off all the substrate except for the deposition area. A Pt plate was used as anode while the n-Si substrate was connected as cathode. A current density of 100 mA/$cm^2$ was maintained between the two electrodes. Film thickness was adjusted as 150 nm by deposition time.

The *I–V* characteristics of the devices were measured in the temperature range of 80–320 K using a temperature cryostat of Janes vpf-475, which enables us to make measurements in the temperature range of 80–320 K, and a Keithly 220 programmable constant current source and a Keithly 199 dmm/scanner under dark conditions. The *C–V* measurements were performed using an HP 4192A LF impedance analyzer. The sample temperature was always monitored by using a copper–constantan thermocouple and a lakeshore 321 auto-tuning temperature controller with sensitivity better than ±0.1 K. All measurements were carried out with the help of a microcomputer through an IEEE-488 AC/DC converter card.

## 3. Results and discussion

The electrical characterizations of the devices were obtained through the *I–V* and *C–V* measurements in the temperature range of 80–320 K by steps of 20 K. The TE theory explains the current flow mechanism across the MS interface in ideal conditions. According to the TE theory [1–4], the current in Schottky contacts can be expressed as:

$$I = I_0 \exp\left(\frac{qV}{nkT}\right)\left[1 - \exp\left(-\frac{qV}{kT}\right)\right] \quad (1)$$

where $I_0$ is the saturation current derived from the straight line intercept of ln $I$ at zero bias and is given by:

$$I_0 = AA^*T^2 \exp\left(-\frac{q\Phi_{bo}}{kT}\right)[0, 1] \quad (2)$$

where $q$ is the electron charge, $V$ is the definite forward-bias voltage, $A$ is the effective diode area, $k$ is the Boltzmann constant ($8.625 \times 10^{-5}$ eV/K), $T$ is the absolute temperature, $A^*$ the Richardson constant of 112 A $cm^{-2}$ $K^{-2}$ for n-type Si [1,3,35], $\Phi_{bo}$ is the effective barrier height at zero bias (which is defined by Eq. (2)), and $n$ is the ideality factor which is a measure of conformity of the diode for the pure TE or characteristic for an ideal Schottky diode. The ideality factor is obtained from the slope of the linear region of the forward bias ln *I–V* plot and it can be written from Eq. (1) as:

$$n = \frac{q}{kT}\frac{dV}{d(\ln I)} \quad (3)$$

The ideality factor, which is introduced to take into account the deviation of the experimental *I–V* data from the ideal thermionic emission model, is close to unity in relatively high temperature region.

The reverse and forward bias *I–V* plots of the Cr/n-type Si Schottky contacts in the temperature range of 80–320 K are given in Fig. 1. The experimental values of $\Phi_{bo}$ and $n$ were determined from Eqs. (2) and (3), respectively, and are shown in Table 1 and Fig. 2. As seen in Table 1 and Fig. 2, the values of zero-bias barrier height $\Phi_{bo}$ and $n$ for the Cr/n-type Si Schottky contacts range from 0.32 eV and 2.26 (at 80 K) to 0.69 eV and 1.21 (at 320 K), respectively. Both parameters strongly depend on temperature. $\Phi_{bo}$ increases while $n$ decreases with increasing temperature. The mean barrier heights obtained from both plots are appropriate with each other. The values of $\Phi_{bo}$ increase with increasing temperature, in which there is a positive coefficient that is in contrast to the negative dependence of the temperature coefficient of the band gap for n-type Si [1,3,5]. This is likely due to the laterally inhomogeneous barrier height causing deviations from the thermionic emission which becomes more pronounced as the temperature decreases [3,5,36]. Because the electrons possess a weak kinetic energy $kT$ at low temperature, they prefer to pass the low barriers [36,37]. The dominant BH will increase with the increasing temperature and bias voltage [3,20,36]. Furthermore, an apparent increase in the ideality factors and decrease in the barrier heights at low temperatures are possibly caused by some other effects such as inhomogeneities of interface layer thickness and non-uniformity of the interfacial charges, etc. [36–38].

The capacitance–voltage (*C–V*) measurements are one of the most important non-destructive methods for obtaining information on rectifying Schottky contact interfaces. Thus, the barrier height $\Phi_{C-V}$ values at various temperatures for the Cr/n-type Si Schottky contact have been calculated from its experimental reverse bias $C^{-2}$–*V* characteristics and given in Fig. 3. The experimental values of $\Phi_{C-V}$ as a function of the temperature are indicated

**Table 1**
Temperature dependent values of various experimental parameters obtained from *I–V* and *C–V* measurements of the Cr/n-Si Schottky contact.

| $T$ (K) | $I_0$ (A) | $n$ (*IV*) | $\Phi_{bo}$ (*IV*) | $\Phi_{bo\,(Norde)}$ (eV) | $\Phi_{b\,(CV)}$ (eV) | $nT$ (K) | $R_{S\,(Norde)}$ (kΩ) |
|---|---|---|---|---|---|---|---|
| 80 | $1.99 \times 10^{-17}$ | 2.26 | 0.32 | 0.49 | 1.09 | 180.56 | 138.93 |
| 100 | $1.89 \times 10^{-17}$ | 1.62 | 0.39 | 0.51 | 1.07 | 162.20 | 41.63 |
| 120 | $1.15 \times 10^{-15}$ | 1.49 | 0.44 | 0.52 | 1.05 | 179.28 | 38.82 |
| 140 | $1.47 \times 10^{-14}$ | 1.42 | 0.48 | 0.54 | 1.02 | 199.22 | 29.31 |
| 160 | $1.34 \times 10^{-12}$ | 1.39 | 0.49 | 0.56 | 0.96 | 223.68 | 21.65 |
| 180 | $1.39 \times 10^{-11}$ | 1.36 | 0.52 | 0.58 | 0.93 | 244.62 | 13.81 |
| 200 | $1.18 \times 10^{-10}$ | 1.34 | 0.55 | 0.59 | 0.86 | 268.20 | 11.23 |
| 220 | $7.61 \times 10^{-10}$ | 1.31 | 0.57 | 0.61 | 0.82 | 288.64 | 8.72 |
| 240 | $3.90 \times 10^{-9}$ | 1.28 | 0.59 | 0.63 | 0.79 | 308.40 | 5.09 |
| 260 | $1.39 \times 10^{-8}$ | 1.26 | 0.62 | 0.65 | 0.77 | 329.16 | 3.34 |
| 280 | $4.63 \times 10^{-8}$ | 1.24 | 0.64 | 0.67 | 0.74 | 349.44 | 1.72 |
| 300 | $1.26 \times 10^{-7}$ | 1.22 | 0.67 | 0.69 | 0.72 | 365.40 | 0.94 |
| 320 | $3.79 \times 10^{-7}$ | 1.21 | 0.69 | 0.70 | 0.72 | 387.52 | 0.46 |

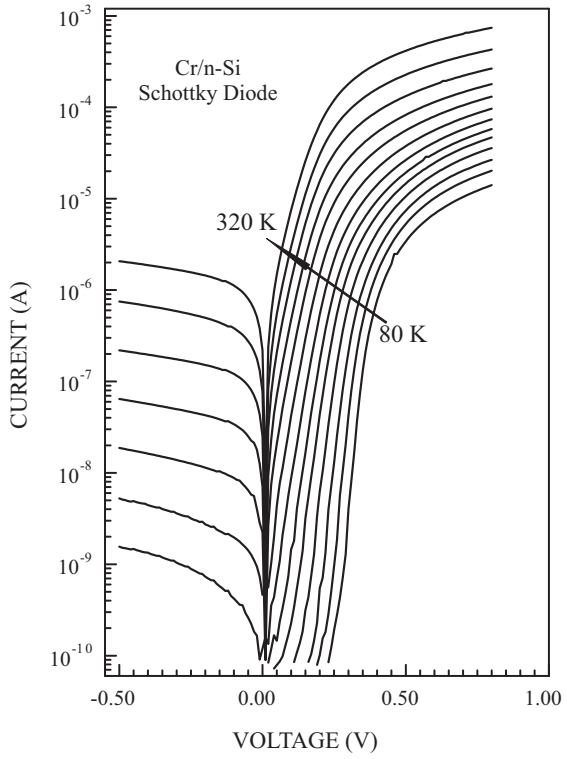


**Fig. 1.** Current–voltage characteristics of the Cr/n-Si Schottky contact at various temperatures.

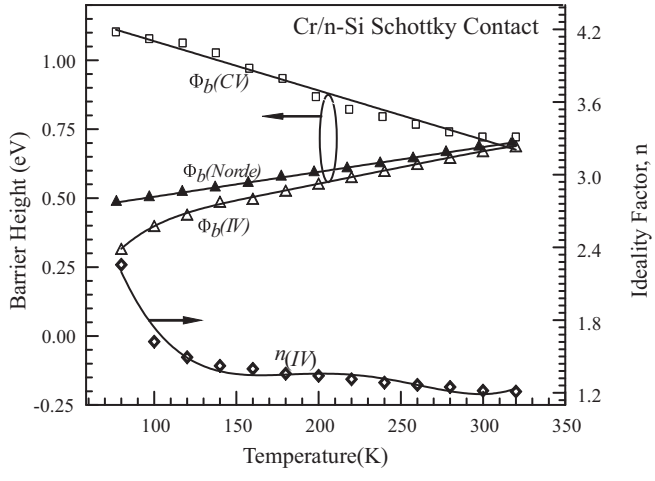


**Fig. 2.** Temperature dependence of the ideality factor and barrier heights for Cr/n-Si Schottky contact.

by open squares in Fig. 2; the $\Phi_{C-V}$ values increased with increasing temperature. As can be seen in Table 1 and Fig. 2, the $\Phi_{C-V}$ values are higher than those derived from the *I–V* measurements as excepted. The experimental values of $\Phi_{C-V}$ range from 1.09 eV at 80 K to 0.72 eV at 320 K. The discrepancy between $\Phi_{CV}$ and $\Phi_{IV}$ can be explained by the existence of excess capacitance and Schottky barrier height inhomogeneities [39–41]. The direct current across the interface is exponentially dependent on barrier height and the current is sensitive to barrier distribution at the interface. Whereas, the capacitance is insensitive to potential fluctuations on a length scale of less than the space charge width that the *C–V* method averages over the whole area. Consequently, the barrier height values obtained from the *C–V* measurement is higher than that obtained from the *I–V* measurements.

As explained above, the values of the ideality factor are not constant with temperature. The temperature dependence of the values of $n$ can be more understood by a plot of $nkT$ versus $kT$, such a plot is given for the Cr/n-type Si Schottky contact in Fig. 4. As shown from Fig. 4, the values of $n$ were found to be inversely proportional with temperature. The temperature dependence of the ideality factor is frequently expressed as $n = n_0 + T_0/T$, where $n_0$ and $T_0$ are constants which are found to be 1.03 and 57.28 K, respectively. $T_0$ is known as a measure of the temperature dependence of the ideality factor. In Fig. 4, the dashed line represents the ideal behavior, $n = 1$, and the experimental data are given by open triangles which were fitted by a straight line parallel to that of the ideal Schottky contact behavior in the temperature range of 100–320 K. A deviation from

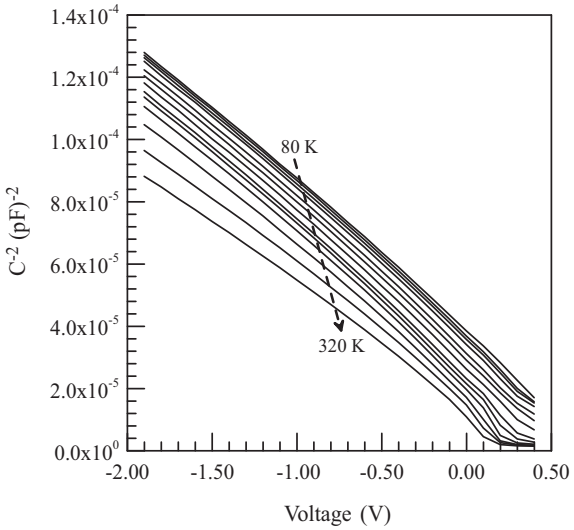


**Fig. 3.** Experimental capacitance–voltage characteristics of a typical Cr/n-Si Schottky contact in the temperature range of 80–320 K.

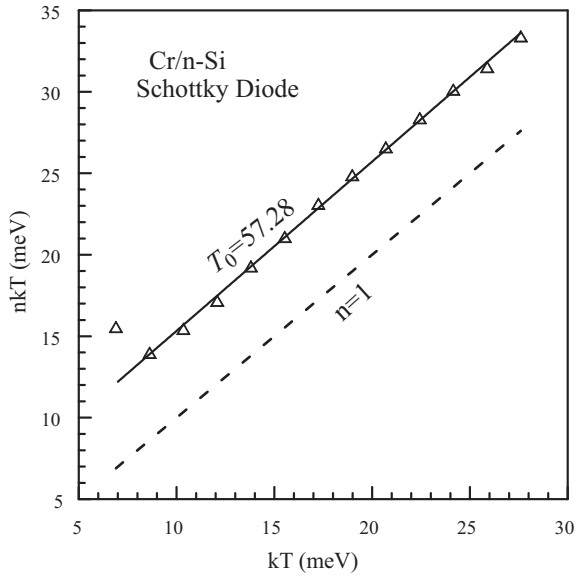


**Fig. 4.** Plot of $nkT$ as a function of $kT$ showing the $T_0$ anomaly from $n = n_o + (T_0/T)$. The dashed line shows the ideal behavior, $n = 1$. The open triangles are the experimental data in the temperature range of 80–320 K in Fig. 1. The value of the slope and the $T_0$ are shown in the figure.

the linearity in the $nkT$ versus $kT$ plot below 100 K was observed. The deviation in the ideality factor in this low temperature region is thought to be caused by the higher value of the ideality factor characterized by the current flow through the distribution of more low SBH patches [42,43].

The saturation current density for $V = 0$, which is used for the Richardson plot, can be written as:

$$\ln\left(\frac{I_0}{T^2}\right) = \ln(AA^*) - \frac{q\Phi_{bo}}{nkT} \tag{4}$$

where $A^*$ is the Richarson constant and $\Phi_{bo}$ is the mean zero voltage barrier height. In Fig. 5, the conventional Richardson plot is introduced. According to the TE theory, the slope of the conventional Richardson plot [$\ln(I_0/T^2)$ versus $1/kT$ plot] should give the barrier height $\Phi_{bo}$. However, the experimental data obtained in this study do not correlate well with a straight line below 160 K. As will be discussed below, this behavior has been interpreted on the basis of standard TE theory and the assumption of a Gaussian distribution of the barrier heights due to the barrier inhomogeneities that persist at the metal–semiconductor interface. As can be seen in Fig. 5, the conventional Richardson plot has a nonlinear part below 160 K which may be caused by the temperature dependence of the BH and ideality factor, particularly pronounced at low temperatures, due to the existence of the surface inhomogeneities of the Si substrate [1–6,14,22]. That is, the observed behavior in the Richardson plot may be due to the spatially inhomogeneous BHs and potential fluctuations at the interface that contains low and high barrier areas [44,45]. The Richardson constant value of $A^* = 4.32 \times 10^{-5}$ A cm$^{-2}$ K$^{-2}$ was determined from the intercept at the ordinate of the experimental plot. This value is much lower than the known value of the Richardson constant for electrons in n-type Si (112 A cm$^{-2}$ K$^{-2}$). This deviation may also be attributed to the spatial inhomogeneous barrier heights and potential fluctuations at the interface formed by low and high barrier areas [20,32,36]. Likewise, the dependence of $\ln(I_0/T^2)$ versus $1/nkT$ (open triangles) is linear in the temperature range of 80–320 K with a slope giving an activation energy of 0.51 eV, and the Richardson constant ($A^*$) is obtained to be equal to $2.02 \times 10^{-3}$ A cm$^{-2}$ K$^{-2}$, which is still significantly lower than the known theoretical value of 112 A cm$^{-2}$ K$^{-2}$ for n type Si [1,3]. As discussed above, the deviation in the Richardson plots may be due to the spatially inhomogeneous BHs and potential fluctuations at the interface that consists of low and high barrier areas, that is, the current through the diode will flow preferentially through the lower barriers in the potential distribution. As was explained by Horváth [46], the value of $A^*$ obtained from the temperature dependence of the $I$–$V$ characteristics may be affected by the lateral inhomogeneity of the barriers, and the fact that it is different from the theoretical value may be connected to a value of the real effective mass that is different from the calculated one.

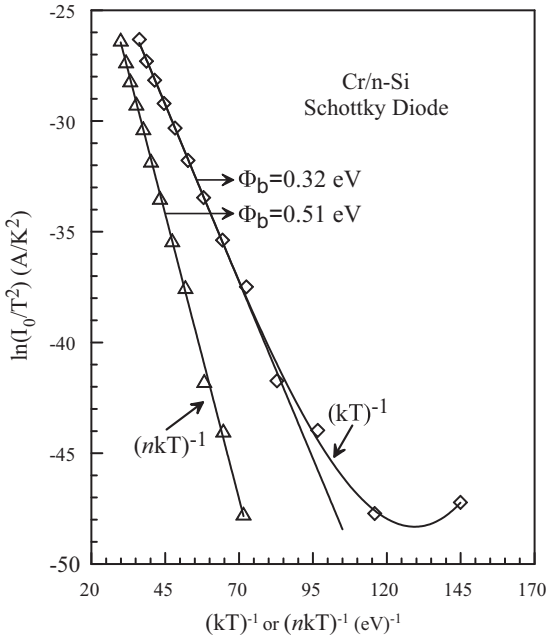


**Fig. 5.** Conventional activation energy ($\ln(I_0/T^2)$ versus $1/kT$) plot (the open squares) and ($\ln(I_0/T^2)$ versus $1/nkT$) plot (the open triangles) for Cr/n-Si Schottky contact.

We assume that the significant decrease in the zero-bias BH and the increase in the ideality factor especially at low temperatures in our samples is possibly caused by the BH inhomogeneities. An analytical potential fluctuation model (a Gaussian distribution of the BHs) introduced by Song et al. [45] can be used to explain the above abnormal behaviors seen in our experimental data. This model is based on spatially inhomogeneous BHs at the interface [4,20,32,45]. Let us assume that the distribution of the BHs is a Gaussian distribution with a mean value $\bar{\Phi}_b$ and a standard deviation $\sigma_s$. The standard deviation is a measure of the barrier homogeneity. The total current in a given forward bias $V$ is then given by:

$$I(V) = I_0 \exp\left(\frac{qV}{n_{ap}kT}\right)\left[1 - \exp\left(-\frac{qV}{kT}\right)\right] \tag{5}$$

with

$$I_0 = AA^*T^2 \exp\left(-\frac{q\Phi_{ap}}{kT}\right) \tag{6}$$

where $\Phi_{ap}$ and $n_{ap}$ are the apparent BH and the apparent ideality factor, respectively, which are given by:

$$\Phi_{ap} = \bar{\Phi}_{bo} - \frac{q\sigma_0^2}{2kT} \tag{7}$$

$$\left(\frac{1}{n_{ap}} - 1\right) = \rho_2 - \frac{q\rho_3}{2kT}. \tag{8}$$

It is assumed that the mean SBH $\bar{\Phi}_b$ and $\sigma_s$ are linearly bias dependent on Gaussian parameters, such as $\bar{\Phi}_b = \bar{\Phi}_{bo} + \rho_2 V$ and standard deviation $\sigma_s = \sigma_{so} + \rho_3 V$, where $\rho_2$ and $\rho_3$ are voltage

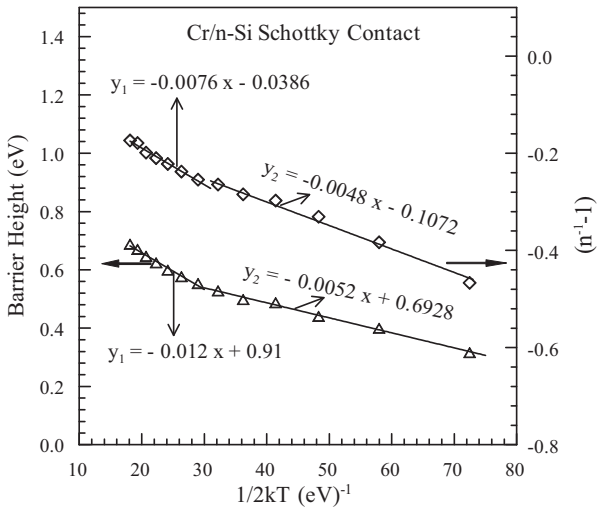


**Fig. 6.** The barrier height $\Phi_{ap}$ (the open triangles) obtained from *I–V* measurements as a function of inverse temperature and the inverse ideality factor $1/n_{ap}$ (the open squares) versus inverse temperature ($1/2kT$) plot for Cr/n-Si Schottky contact.

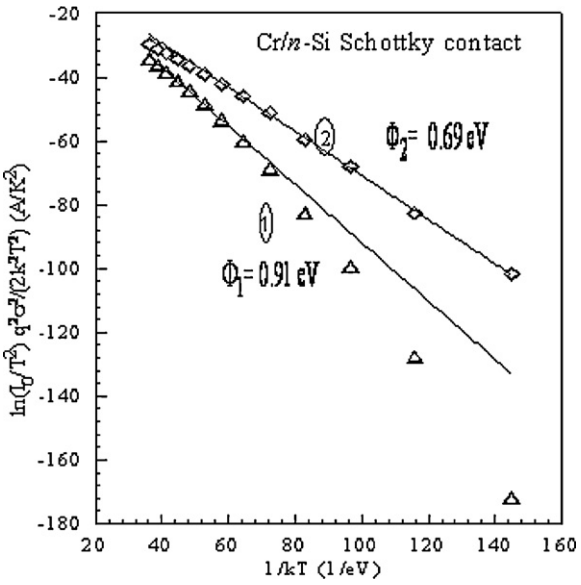


**Fig. 7.** Modified activation energy ($\ln(I_0/T^2) - q^2\sigma_0^2/2k^2T$ versus $1/kT$) plots for Cr/n-Si Schottky contact according to two Gaussian distributions of barrier heights. The plots for zero-bias standard deviation $\sigma_s$ equal to 0.109 V and 0.072 V are shown by open triangles and open squares, respectively. The straight lines 1 and 2 indicate the best fitting of the data in the temperature ranges of 200–320 K and 80–180 K, respectively.

coefficients and they quantify the voltage deformation of the BH distribution. The temperature dependence of $\sigma_s$ is usually small and can be neglected. The experimental $\Phi_{ap}$ versus $1/T$ and $n_{ap}$ versus $1/T$ plots (Fig. 6) drawn by means of the data obtained from Fig. 1 respond to two lines instead of a single straight line with a transition occurring at 180 K. Fitting the experimental data with Eqs. (2) or (6) and with Eq. (3) gives $\Phi_{ap}$ and $n_{ap}$, respectively, which should obey Eqs. (7) and (8). Thus, the plot of $\Phi_{ap}$ versus $1/T$ (Fig. 6) should be a straight line with the intercept at the ordinate determining the zero-bias mean barrier height $\bar{\Phi}_{bo}$ and the slope giving the zero-bias standard deviation $\sigma_s$. The above observations indicate the presence of two Gaussian distributions of barrier heights in the contact area. The intercepts and slopes of these straights lines give two sets of values of $\bar{\Phi}_{bo}$ and $\sigma_s$ as 0.910 eV and 109 mV in the temperature range of 200–320 K (distribution 1), and as 0.693 eV and 72 mV in the temperature range of 80–180 K (distribution 2). As explained above, the standard deviation is a measure of the barrier homogeneity. Thus, the lower value of $\sigma_s$ corresponds to more homogeneous barrier height. However, it was seen that the value of $\sigma_s$ = 109 mV is not small compared to the mean value of $\bar{\Phi}_{bo} = 0.910$ eV, and $\sigma_s$ = 72 mV is not small compared to the mean value of $\bar{\Phi}_{bo} = 0.0693$ eV, too, so it indicates the presence of the interface inhomogeneities. This study therefore shows that the Cr/n-type Si Schottky contact has a double-Gaussian distribution. The existence of a double-Gaussian distribution in the metal–semiconductor contacts can be attributed to the nature of the inhomogeneities themselves in the two cases [32,46]. This may involve the variation in the interface composition/phase, interface quality, electrical charges and non-stoichiometry, etc. They are important enough to electrically influence the *I–V* characteristics of the Schottky contacts, at particularly low temperatures. Thus, the *I–V* measurements at very low temperatures are capable of revealing the nature of barrier inhomogeneities present in the contact area. That is, the existence of second Gaussian distribution at very low temperatures may possibly arise due to some phase change taking place on cooling below a certain temperature. Furthermore, the temperature range covered by each straight-line suggests the regime where corresponding distribution is effective [9].

Similarly the $1/n_{ap}$ versus $1/T$ should also possess different characteristics in the two temperature ranges if the contact contains two barrier height distributions. This is indeed the case (open squares in Fig. 6) as the data clearly fit with two straight lines in the temperature ranges 200–320 K and 80–180 K for Cr/n-type Si Schottky contact. The intercept and slope of the straight lines in $1/n_{ap}$ versus $1/T$ plot give the voltage coefficient $\rho_2$ and $\rho_3$, respectively. The values of $\rho_2$ obtained from the intercepts of the experimental $1/n_{ap}$ versus $1/T$ plot (Fig. 6) are 0.0386 V in the temperature range of 200–320 K (distribution 1), and 0.1072 in the temperature range of 80–180 K (distribution 2), whereas the values of $\rho_3$ from the slopes are −0.0076 V in 200–320 K range and −0.0048 V in 80–180 K temperature ranges. The linear behavior of this plot demonstrates that the ideality factor does indeed express the voltage deformation of the Gaussian distribution of the BH. As can be seen from the $1/n_{ap}$ versus $1/T$ plot, $\rho_3$ value or the slope of the distribution 1 is larger than that of the distribution 2. Therefore, we may point out that the distribution 1 is a wider and relatively higher barrier height with the bias coefficients $\rho_2$ and $\rho_3$ being smaller and larger, respectively. Consequently, we can say that the distribution 2 at low temperatures may possibly arise due to some phase change taking place on cooling below a certain temperature.

Moreover, the activation energy plot, [$\ln(I_0/T^2)$ versus $1/kT$], shows nonlinearity at low temperatures, as stated above. To explain these discrepancies according to the Gaussian distribution of the BH, for a modified activation energy plot, Eq. (6) can be rewritten by combining with Eq. (7) as:

$$\ln\left(\frac{I_0}{T^2}\right) - \left(\frac{q^2\sigma_s^2}{2k^2T^2}\right) = \ln(AA^*) - \frac{q\bar{\Phi}_{bo}}{kT} \quad (9)$$

The term $\ln(I_0/T^2) - q^2\sigma_0^2/2k^2T^2$ is calculated for both values of $\sigma_s$, associated with the Gaussian distributions of barrier heights in the temperature ranges of 80–180 K and 200–320 K. As can be seen, the values of $\bar{\Phi}_{bo} = 0.69$ eV (in the range of 80–180 K) and 0.91 eV (in the range of 200–320 K) obtained from Fig. 7 are the same as the $\bar{\Phi}_{bo}$ values obtained from the $\bar{\Phi}_{ap}$ versus $(2kT)^{-1}$ plot in Fig. 6. Likewise, the mean BH values obtained from Figs. 5–7 in high temperature ranges are very close to the BH values obtained from $C^{-2}$–$V$ characteristics. This indicates that the BH measured by the *C–V* experiment is always close to the weighed arithmetic average of the Schottky barrier heights in the inhomogeneous metal–semiconductor contacts.

The current generating mechanisms such as thermionic field emission (TFE) or recombination may cause the decrease in the barrier height and the increase in the ideality factor with decreasing temperature [1–3,22]. It is indicative of deviation from the pure thermionic emission (TE) theory and possibly the TFE mechanism warrants consideration. Therefore, thermionic-field emission is likely the mechanism for efficiently low temperature forward current flow. That is, the TFE cannot possibly account for the observed high ideality factor values. The parameter that determines the relative importance of tunneling and thermionic emission is given by [3,29].

$$E_{oo} = \frac{h}{4\pi}\left(\frac{N_D}{m_e^* \varepsilon_s \varepsilon_0}\right)^{1/2} \tag{10}$$

where $E_{oo}$ is the characteristic tunneling energy that is related to the transmission probability ($= h/4\pi(N_D/m_e^*\varepsilon_s\varepsilon_0)^{1/2}$), $m_e^*$ (=0.98 $m_o$) is the effective mass for electrons [1–3], $N_D$ is the ionized donor density of the n-Si obtained by temperature dependent $C$–$V$ measurement and $\varepsilon_s$ (=11.8$\varepsilon_0$) is the permittivity of Si [1–3]. According to the theory, field emission (FE) becomes important when $E_{oo} \gg kT$ whereas TFE dominates when $E_{oo} \approx kT$ and TE is crucial if $E_{oo} \ll kT$. The values of $E_{oo}$ are equal to 0.0794 and 0.0852 meV at 80 and 320 K, respectively. However, the values of $kT/q$ are equal to 6.90 and 27.60 meV at 80 and 320 K, respectively. Therefore, we can express that all over the temperature range TE is the dominant current mechanism and the possibility of the FE and TFE can easily be ruled out [3,22].

It has been observed that the voltage drop caused a non-ideal behavior at all temperatures at a high voltage region, which is series resistance region. According to the TE theory, the forward bias $I$–$V$ characteristics of a SBD with the series resistance can be expressed as [1,3]:

$$I = I_0 \exp\left(\frac{q(V - IR_S)}{nkT}\right) \tag{11}$$

where $R_S$ is the series resistance and the $IR_S$ term is the voltage drop across the series resistance of the diode. Norde proposed an method to determine the values of the series resistance and barrier height [47]. The following function (Norde's function, $F(V)$) has been defined in the modified Norde's method [47]:

$$F(V) = \frac{V}{\gamma} - \frac{kT}{q}\ln\left(\frac{I(V)}{AA^*T^2}\right) \tag{12}$$

where $\gamma$ is a first integer (dimensionless) greater than $n$, and $I(V)$ is the current obtained from the current–voltage curve. Once the minimum of the $F$ versus $V$ plot is determined, the value of barrier height can be obtained from Eq. (12):

$$\Phi_b = F(V_{min}) + \frac{V_{min}}{2} - \frac{kT}{q} \tag{13}$$

where $F(V_{min})$ is the minimum value of $F(V)$ and $V_{min}$ is the corresponding voltage. A plot of $F(V)$ versus $V$ for the Cr/n-Si Schottky contact at different temperatures is shown in Fig. 8. According to Eq. (13), the barrier height values obtained by the Norde's method for the Cr/n-Si Schottky contact is given in Fig. 2 (indicated by closed triangles) and Table 1. As can be seen in Fig. 2 and Table 1, the BHs obtained by Norde's method are in good agreement with the values obtained by the $I$–$V$ method. The increase in the BHs at higher temperatures may be due to the interface states and chemical reactions between metal and semiconductor at the interface. As explained above, to compare the effective Schottky barrier height of contacts, the Norde method was also employed [47] because high series resistance ($R_S$) can hinder an accurate evaluation of barrier height from the standard ln $I$–$V$ plot. The value of the series resistance can be obtained from the Norde's method for the Cr/n-type Si Schottky structure. From the Norde's functions, the value of the $R_S$ is determined as [47]:

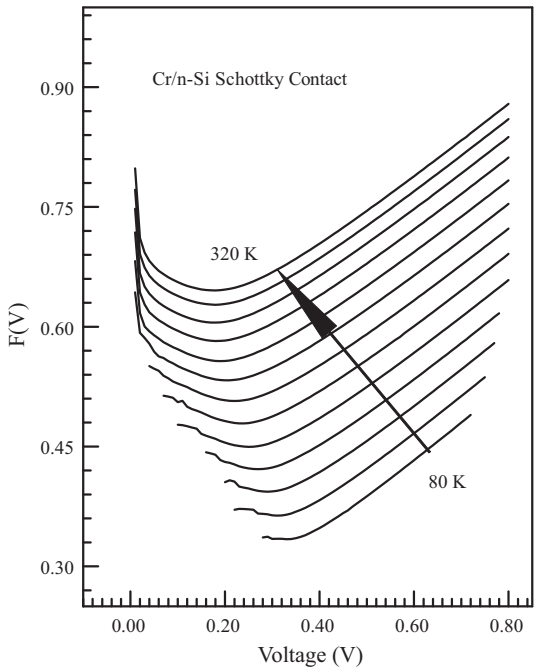


**Fig. 8.** $F(V)$ versus $V$ plot of the Cr/n-Si Schottky contact at various temperature.

$$R_S = \frac{(2-n)kT}{qI_{min}} \tag{14}$$

where $I_{min}$ is the corresponding current at $V = V_{min}$ where the function $F(V)$ exhibits a minimum. From the $F(V)$–$V$ plots, the values of the series resistance ($R_S$) of the Cr/n-type Si Schottky contact given in Fig. 9 and Table 1 have been determined as 0.466 kΩ at 320 K and 138.93 kΩ at 80 K, respectively. As can be seen in Table 1, the SBH has decreased and the series resistance has increased with decreasing temperature. The increase of the Cr/n-type Si Schottky contact resistivity causes an increase of $R_S$, which leads to a down-

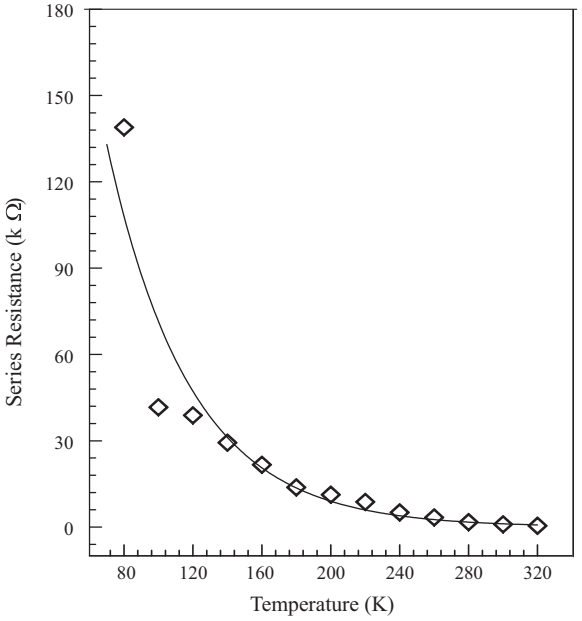


**Fig. 9.** Temperature dependence of the resistances obtained from the Norde's function of Cr/n-Si Schottky contact.

ward *I–V* curve at high voltages. That is, when the temperature increases, more and more electrons have sufficient energy to surmount the higher barrier. The high values of the series resistance can be attributed to the freeze-out of carriers at low temperatures.

## 4. Conclusions

In this study, the *I–V* and *C–V* characteristics of the Cr/n-Si Schottky contact prepared by electrodeposition technique were investigated in the temperature range of 80–320 K. The basic diode parameters such as ideality factor and barrier height were extracted from these electrical measurements. The estimated barrier height $\Phi_{bo}$ and the ideality factor $n$ assuming TE mechanism show strong temperature dependence. It was seen that the ideality factors increased and the barrier heights decreased with decreasing temperature. It was ascribed to the barrier inhomogeneity at the metal/semiconductor interface. The electrical measurements show that the temperature-dependent current–voltage characteristics of the Cr/n-Si Schottky contacts can be explained by the double Gaussian distribution of barrier heights. The activation energy $\ln(I_s/T^2)$ versus $1/(nkT)$ plot yielded a straight line with an effective barrier height value of 0.51 eV. It has been seen that the analysis under the Gaussian distribution of BH model or $n$ versus $1/T$ plot show two slope behavior and serve as the basis for the proposal of the presence of a double Gaussian distribution of BHs at the MS interface. The modified $\ln(I_0/T^2) - q^2\sigma_0^2/2k^2T^2$ versus $1/kT$ plots yielded a zero bias mean BH $\bar{\Phi}_{bo}$ of 0.69 eV in the range of 80–180 K (distribution 2) and 0.91 eV in the range of 200–320 K (distribution 1). These values are in close agreement with the mean BHs obtained from the $\Phi_{ap}$ versus $1/(2kT)$ plot in Fig. 6. In addition, the series resistance and the barrier height values were also calculated with the Norde's method, and it was seen that the BHs obtained by the Norde's method are in good agreement with the values obtained by the *I–V* method. In summary this study, it can be said that this Cr/n-Si Schottky contacts show good diode behavior. According to the electrical characterization, in the future, it can be used rectifying contacts, integrated circuits, the other electronic devices and so on. Therefore, due to the technological importance of metal–semiconductor structures, the foundation of the electronics industry is the semiconductor device.

## References


[1] M. Sze, Physics of Semiconductor Devices, 2nd ed., Wiley, New York, 1981, p. 850.
[2] B. Abay, J. Alloys Compd. 506 (2010) 51.
[3] E.H. Rhoderick, R.H. Williams, Metal–Semiconductor Contacts, 2nd ed., Clarendon, Oxford, 1988.
[4] M. Soylu, B. Abay, Microelectron. Eng. 86 (2009) 88.
[5] N. Yildirim, H. Korkut, A. Turut, Eur. Phys. J. Appl. Phys. 45 (2009) 10302.
[6] Y. Du, Q.X. Yuan, J. Alloys Compd. 492 (2010) 548.
[7] A. Sellai, M. Mamo, Appl. Phys. A 89 (2007) 503.
[8] M. Mamora, A. Sellai, J. Vac. Sci. Technol. A 26 (4) (2008) 705.
[9] P.G. Mc Cafferty, A. Sellai, P. Dawson, H. Elasd, Solid State Electron. 39 (1996) 583.
[10] G.S. Chung, K.S. Kim, F. Yakuphanoglu, J. Alloys Compd. 507 (2010) 508.
[11] W.C. Huang, C.T. Horng, Appl. Surf. Sci. 257 (2011) 3565.
[12] N. Yıldırım, A. Türüt, V. Türüt, Microelectron. Eng. 87 (2010) 2225.
[13] B. Güzeldir, M. Sağlam, A. Ateş, J. Alloys Compd. 506 (2010) 388.
[14] S. Asubay, Ö. Güllü, A. Türüt, Vacuum 83 (2009) 1470.
[15] F.E. Cimili, H. Efeoğlu, M. Sağlam, A. Türüt, J. Mater. Sci.: Mater. Electron. 20 (2009) 105.
[16] L Wang, M.I. Nathan, T.H. Lim, M.A. Khan, Q. Chen, Appl. Phys. Lett. 68 (1996) 1267.
[17] V. Baranwal, S. Kumar, A.C. Pandey, D. Kanjilal, J. Alloys Compd. 480 (2009) 962.
[18] M. Mamor, J. Phys.: Condens. Matter 21 (2009) 335802.
[19] T. Kılıçoğlu, M.E. Aydın, G. Topal, M.A. Ebeoğlu, H. Saygılı, Synth. Met. 157 (2007) 540.
[20] J.H. Werner, H.H. Güttler, J. Appl. Phys. 69 (1991) 1522.
[21] S. Chand, J. Kumar, J. Appl. Phys. 82 (1997) 5005.
[22] Ş. Karataş, Ş. Altındal, Mater. Sci. Eng. B 122 (2005) 133.
[23] M. Sağlam, A. Ateş, B. Güzeldir, A. Astam, M.A. Yıldırım, J. Alloys Compd. 484 (2009) 570.
[24] M.E. Kiziroglou, A.A. Zhukov, M. Abdelsalam, X. Li, P.A.J. de Groot, P.N. Bartlett, C.H. de Groot, IEEE Trans. Magn. 41 (2005) 2639.
[25] Z.L. Bao, K.L. Kavanagha, J. Vac. Sci. Technol. B 24 (2006) 2138.
[26] A. Eftekhari, Microelectron. Eng. 69 (2003) 17.
[27] H. Hasegawa, Jpn. J. Appl. Phys. 38 (1999) 1098.
[28] S. Kasai, H. Hasegawa, Appl. Surf. Sci. 175–176 (2001) 181.
[29] R. Sharma, J. Electron Devices 8 (2010) 286.
[30] Ç. Nuhoğlu, Y. Gülen, Vacuum 84 (2010) 812.
[31] Ş. Karataş, M. Çakar, Synth. Met. 159 (2009) 347.
[32] S. Chand, J. Kumar, Semicond. Sci. Technol. 10 (1995) 1680.
[33] B. Tatar, A.E. Bulgurcuoğlu, P. Gökdemir, P. Aydoğan, D. Yılmazer, O. Özdemir, K. Kutlu, Int. J. Hydrogen Energy 34 (2009) 5208.
[34] Yi. Zhou, D. Wang, C. Ahyi, C.C. Tin, J. Williams, M. Park, N.M. Williams, A. Hanser, E.A. Preble, J. Appl. Phys. 101 (2007) 024506.
[35] G. Güler, Ö. Güllü, Ş. Karataş, Ö.F. Bakkaloğlu, J. Phys.: Conf. Ser. 153 (2009) 012054.
[36] S. Duman, Semicond. Sci. Technol. 23 (2008) 075042.
[37] H. Benmaza, B. Akkal, H. Abid, M.J. Bluet, M. Anani, Z. Bensaad, Microelectron. J. 39 (2008) 80.
[38] Ş. Altindal, S. Karadeniz, N. Tuğluoğlu, A. Tataroğlu, Solid State Electron. 47 (2003) 1847.
[39] F. Yakuphanoglu, B.F. Senkal, J. Phys. Chem. C 111 (2007) 1840.
[40] S. Chattopadhyay, L.K. Bera, S.K. Ray, P.K. Bose, D. Dentel, L. Kubler, J. Mater. Sci. Mater. Electron. 9 (6) (1998) 403.
[41] Ö Güllü, M. Biber, A. Türüt, J. Mater. Sci.: Mater. Electron. 19 (2008) 986.
[42] J.P. Sullivan, R.T. Tung, M.R. Pinto, W.R. Graham, J. Appl. Phys. 70 (1991) 7403.
[43] R.T. Tung, Phys. Rev. B 45 (1992) 13509.
[44] J. Osvald, Semicond. Sci. Technol. 18 (2003) L24.
[45] G.P. Ru, R.L. Van Meirhaeghe, S. Forment, Y.L. Jiang, X.P. Qu, S. Zhu, B.Z. Li, Solid State Electron. 49 (2005) 606;
Y.P. Song, R.L. Van Meirhaeghe, W.H. Laflere, F. Cardon, Solid State Electron. 29 (1986) 633.
[46] Zs.J. Horvath, Solid State Electron. 39 (1996) 176;
H. Altuntaş, Ş. Altındal, H. Shtrikman, S. Özçelik, Microelectron. Reliab. 49 (2009) 904.
[47] H. Norde, J. Appl. Phys. 50 (1979) 5052.